Electronic Structures of Hexacyanometalate Complexes

John J. Alexander[1a] and Harry B. Gray[1b]

Contribution from the Department of Chemistry, Columbia University, New York, New York 10027, and Contribution No. 3576 from the Gates and Crellin Laboratories of Chemistry,[1c] California Institute of Technology, Pasadena, California 91109. *Received October 30, 1967*

Abstract: Electronic energy levels for hexacyano complexes of the first-row transition metals calculated using a modified Wolfsberg–Helmholz approach are employed to assign the bands in the electronic spectra in these complexes and some of their second- and third-row analogs In particular, the controversial first ligand-to-metal charge-transfer band in ferricyanide is shown to be of $\sigma \rightarrow \pi$ type. Spectral measurements in solids and liquid solutions at 300°K and for frozen solutions at 77°K have been made and the envelopes analyzed into Gaussian components in order to reveal the LaPorte-forbidden or -allowed character of the transitions. As part of this study, the hitherto unknown $Os(CN)_6^{3-}$ was isolated and characterized as a n-Bu_4N^+ salt. Independence of the ligand-field parameter Δ from metal oxidation state and constancy of orbital electronegativity for transition metals in a periodic group are shown to be consequences of the electronic structures of cyano complexes and others in which the ligands are capable of back-bonding to π^* orbitals.

Complexes of the transition metals with ligands having low-lying unfilled antibonding orbitals of π symmetry display several interesting properties; for example, low oxidation states of the central metal are stabilized; also, even in first-row complexes, the magnetic behavior is of the "low-spin" type. In the particular case of cyanide and carbonyl ligands, there seems to be an unexpectedly small dependence of the ligand-field parameter Δ on the oxidation state of the central metal. To illustrate, Δ changes from 33,800 to 35,000 cm^{-1} in going from $Fe(CN)_6^{4-}$ to $Fe(CN)_6^{3-}$, whereas the comparable values for the respective aquo complexes are 10,000 and 14,000 cm^{-1}. Again, whereas in halide complexes of the first row Δ decreases from Ti to Co for a series having the same oxidation state, cyano complexes display just the opposite trend, having $\Delta \simeq 22{,}000$ cm^{-1} for $Ti(CN)_6^{3-}$ and $\Delta \sim 35{,}000$ cm^{-1} for $Co(CN)_6^{3-}$.

A discussion of the electronic structures of hexacyano complexes requires the calculation of appropriate energy level schemes and the assignment of the various bands of the electronic spectra by reference to such level orderings. Various attempts[2-8] have been made to do this, none with much success. The d^6 cyanides of several metals have been discussed[9] in terms of an estimated energy level scheme and assignments given for the important spectral bands. Also, some controversy[10-12] has occurred over the nature of the charge-transfer bands of ferricyanide. However, no systematic effort to interpret the electronic transitions of first-row hexacyanides is yet available; a recent review[13] of cyanide chemistry has called attention to the absence of a consistent MO explanation of these excitations.

We have, therefore, calculated energy level schemes for the first-row cyanides using a modified[14] Wolfsberg–Helmholz[15] model; on the basis of the derived schemes we have assigned the observed electronic transitions and obtained evidence of the consistency of our assignments through spectra measured at 77°K which reveal the Laporte-allowed or -forbidden character of the bands. In analogy to first-row species, several second- and third-row hexacyano complexes are also discussed. In this connection, we have isolated and investigated $[n\text{-}Bu_4N]_3[Os(CN)_6]$, which contains the hitherto unknown third-row analog of ferricyanide.

Experimental Section

Preparation of Hexacyanide Complexes. Standard literature preparations were employed for $K_3Co(CN)_6$,[16] $K_3Mn(CN)_6$,[17] and $H_4Fe(CN)_6$;[18] these compounds were purified by recrystallization from water. Baker and Adamson reagent grade $K_3Fe(CN)_6$ and $K_4Fe(CN)_6 \cdot 3H_2O$ were recrystallized from water before use. The complexes $K_3Ir(CN)_6$, $K_3Rh(CN)_6$, and $K_4Os(CN)_6 \cdot 3H_2O$ were obtained from City Chemical Co.

The salt $K_4Mn(CN)_6 \cdot 3H_2O$ was prepared by a modification of the method of Figgis;[19] powdered $MnCl_2 \cdot 4H_2O$ was placed in a glass-stoppered erlenmeyer flask which was flushed with nitrogen. An appropriate volume of boiling 2 M KCN solution was added and the flask stoppered tightly. Initially, a green, powdery precipitate of $KMn(CN)_3$[20] was formed, but, after standing overnight, blue-black crystals of $K_4Mn(CN)_6 \cdot 3H_2O$ were present. They were collected on a Büchner funnel, washed with 50% EtOH and ether, dried, and stored under vacuum. All solutions for spectral measurements were made by dissolving weighed quantities of the crystals in KCN solutions which were boiled, deaerated, and cooled.

Several attempts at literature preparations[21,22] of $K_3Cr(CN)_6$·

(1) (a) Columbia University; National Science Foundation Predoctoral Fellow 1965–1967; (b) California Institute of Technology.
(2) C. Spanjaard and G. Berthier, *J. Chim. Phys.*, **58**, 169 (1961).
(3) G. Berthier, P. Millie, and A. Veillard, *ibid.*, **62**, 20 (1965).
(4) F. J. Gilde and M. I. Ban, *Acta Univ. Szeged. Acta Phys. Chem.*, **3**, 42 (1957).
(5) M. I. Ban, *Acta Chim. Acad. Sci. Hung.*, **19**, 459 (1959).
(6) M. I. Ban and E. Harvath, *Acta Univ. Szeged. Acta Phys. Chem.*, **5** (3), 34 (1959).
(7) M. I. Ban, S. Fenyi, and F. J. Gilde, *Z. Physik. Chem.* (Leipzig), **221**, 193 (1962).
(8) F. J. Gilde, *Acta Univ. Szeged. Acta Phys. Chem.*, **6** (1), 3 (1960).
(9) H. B. Gray and N. A. Beach, *J. Am. Chem. Soc.*, **85**, 2922 (1963).
(10) (a) C. S. Naiman, *J. Chem. Phys.*, **35**, 323 (1961); (b) *ibid.*, **39**, 1900 (1963).
(11) G. B. Basu and R. L. Belford, *ibid.*, **37**, 1933 (1962).
(12) P. J. Stephens, *Inorg. Chem.*, 4, 1690 (1965); P. N. Schatz, A. J. McCaffery, W. Suëtaka, G. N. Henning, A. B. Ritchie, and P. J. Stephens, *J. Chem. Phys.*, **45**, 722 (1966).
(13) B. M. Chadwick and A. G. Sharpe, *Advan. Inorg. Chem. Radiochem.*, **8**, 830 (1966).
(14) C. J. Ballhausen and H. B. Gray, *Inorg. Chem.*, 1, 111 (1962).
(15) M. Wolfsberg and L. Helmholz, *J. Chem. Phys.*, 20, 837 (1952).
(16) J. H. Bigelow, *Inorg. Syn.*, 2, 225 (1946).
(17) J. A. Lower and W. C. Fernelius, *ibid.*, 2, 213 (1946).
(18) G. Brauer, "Handbook of Preparative Inorganic Chemistry," Academic Press Inc., New York, N. Y., 1963, p 1509.
(19) B. N. Figgis, *Trans. Faraday Soc.*, **57**, 298 (1964).
(20) A. Descamps, *Ann. Chim.* (Paris), **24**, 178 (1881).
(21) F. Cruser and E. Miller, *J. Am. Chem. Soc.*, **28**, 1132 (1906).
(22) J. H. Bigelow, *Inorg. Syn.*, 2, 203 (1946).

$3H_2O$ led to products contaminated with K_2CrO_4. Consequently, a solution of $K_4Cr(CN)_6$[23] was prepared and allowed to oxidize in air. Yellow crystals formed on evaporation; these were collected, washed, and recrystallized.

The hexacyano complex of V(III) was prepared in the following modification of the procedure of Locke and Edwards.[24a] Water and 50% ethanol, which were boiled and degassed by bubbling nitrogen while cooling, were placed in an ice bath for 1 hr. In an inert nitrogen atmosphere 5 g of VCl_3 (Alpha Inorganics research chemical used as received) was dissolved in the minimum possible volume of cold water, yielding a yellow-brown solution which turned green on acidification with a few drops of HCl. KCN (19 g, 1.5 times the theoretical amount) was dissolved in a minimum volume of water; the V(III) solution was slowly added with stirring to give a blue-violet solution which was then filtered. Ethanol (30 ml) was added to the filtrate and the beaker cooled in ice water.

A blackish purple precipitate formed on the walls and bottom of the vessel; it was collected on a frit and placed in a vacuum overnight. By morning, it had decomposed to a green and black powder. The filtrate left overnight in the inert atmosphere deposited a yellow-brown, shiny precipitate which contained small brick-red crystals. These two substances could be separated by flotation in ethanol; the red crystals were thus collected, dried, and stored under N_2. A mull spectrum gave agreement with the results of aqueous solutions (*vide infra*). The crystals turned brown after a week. Attempts to repeat the preparation were unsuccessful.

Anal. Calcd for $K_3V(CN)_6 \cdot 3H_2O$ + 0.15KCN: C, 19,80; N, 23.10; H, 1.00. Calcd for $K_3V(CN)_6 \cdot 3H_2O$: C, 19.25; N, 21.38; H, 1.87. Found: C, 19.82; N, 23.11; H, 0.95.

The analytical results found for our red crystalline product would equally well support its formulation as the complex $K_4V(CN)_7 \cdot 2H_2O$. Indeed, seven coordination has been suggested[13] recently in investigations of complexes of vanadium with cyanide. Since all our spectroscopic data are consistent with an octahedral species, we shall continue to refer to the complex in question as $V(CN)_6^{3-}$ pending more conclusive structural evidence. Investigations by R. A. Levenson bearing on this point are now in progress at the California Institute of Technology.

Aqueous solutions of $V(CN)_6^{3-}$ were prepared by dissolving weighted amounts of VCl_3 in an appropriate volume of degassed 1.5 *M* KCN solution in an inert atmosphere. The resulting solution was purple and showed an intense absorption at 5780 Å which faded rapidly to give a red-orange solution whose spectrum matched that of the scarlet crystals in mull and in 1.5 *M* KCN solution. After about 0.5 hr, these solutions decomposed to give a brown, flocculent precipitate, probably $V(OH)_3$.

Tetrabutylammonium Salts for Low-Temperature Spectra. [*n*-$Bu_4N]_3[Co(CN)_6]$ and [*n*-$Bu_4N]_3[Fe(CN)_6]$ were prepared by passing 1-g quantities of the potassium salts over 30 g of Amberlite IR-12, which had previously been washed with 10% HCl followed by repeated washings with distilled water until the washings gave no precipitate with 0.1 *M* $AgNO_3$ solution. The acids thus obtained were immediately titrated with 25% tetra-*n*-butylammonium hydroxide in methanol using phenophthalein as an indicator. The water and methanol were stripped at 60° and the compounds dried over P_2O_5. The salts could be recrystallized from 50% EtOH by cooling and addition of ether. The crystals so obtained had to be freed from solvent immediately by placing them in a desiccator over P_2O_5 and pumping under high vacuum since otherwise they reverted to oils. Tetramethylammonium salts of several anions were also prepared in this way and found to be insoluble in EPA.

The above procedure caused the ferrocyanide ion to be oxidized cleanly to ferricyanide and thus was used to prepare the hitherto unknown osmicyanide as the salt [*n*-$Bu_4N]_3[Os(CN)_6]$ from $K_4Os(CN)_6$. The compound is a yellow powder. It may be recrystallized from dichloromethane–hexane to give yellow plates. A previous report[24b] of a blue solution obtained on air oxidation of $Os(CN)_6^{4-}$ is very probably the osmium analog of Prussian blue.

Anal. Calcd for [*n*-$Bu_4N]_3[Os(CN)_6]$: C, 60.49; N, 11.75; H, 10.07; Os, 17.69. Found: C, 60.64; N, 11.40; H, 10.22; Os, 17.82.

Magnetic susceptibility measurements at 296°K gave μ_{eff} = 2.12 BM, consistent with the expected $(t_{2g})^5 = {}^2T_{2g}$ ground state.

Physical Measurements. Ultraviolet and Visible Spectra. Solutions of complexes in various solvents and employing 1-cm or 0.1-mm quartz cells were scanned using a Cary Model 14 spectrophotometer. For the region 220–190 mμ, the sample and cell compartments, as well as the lamp and monochromator, were flushed with dry N_2 gas.

Mull spectra were recorded by grinding the salt of interest in an agate mortar, mulling with Nujol, and spreading a layer of the mull on a strip of filter paper which was placed in the sample beam. A strip of filter paper with Nujol was placed in the reference beam.

Low-Temperature Spectra. All complexes for which tetra-*n*-butylammonium salts could be obtained were dissolved in EPA for determination of low-temperature spectra. EPA, obtained from the Olin-Matheson Co. or the Hartmann-Leddon Co., is a mixture of ethanol, isopentane, and ether in the ratio 2:5:5 by volume. This solvent, if dry, forms a clear glass which is transparent in the region 700–210 mμ at the temperature of liquid N_2.

The spectrum at 77°K of $H_4Fe(CN)_6$ was obtained in 7:3 isopentane–butanol, which also forms a clear glass transparent in the region of interest. Since the pure tetra-*n*-butylammonium salts of $Cr(CN)_6^{3-}$ and $Mn(CN)_6^{3-}$ could not be prepared, the low-temperature spectra of their potassium salts were obtained at 143°K in 2:1 ethylene glycol–water (in the latter case, the solvent was saturated with KCN). This solvent system has a weak absorption at *ca.* 2550 Å which can be compensated for in solutions of complexes by subtracting the background absorption of the ethylene glycol. This procedure was tested by verifying that the same quantitative results were obtained for $Fe(CN)_6^{3-}$, both in EPA and in 2:1 ethylene glycol–water. The procedure used for obtaining low-temperature glass spectra has been given previously.[25] For the ethylene glycol–water glass, an *n*-pentane slush was used as the coolant since this solvent cracks at liquid nitrogen temperature.

No correction was made for solvent contraction in isopentane–butanol and ethylene glycol–water since no data are available for these systems. Because the quartz of the low-temperature cell had a cut-off point of 240 mμ, no measurements were made beyond this point.

Infrared Spectra. Ir spectra of Nujol mulls were taken on a Perkin-Elmer 421 grating spectrophotometer between sodium chloride plates. Solution spectra of some tetraalkylammonium salts in spectral grade chloroform were obtained using cells with sodium chloride windows. Integrated intensity measurements were performed on a Beckman IR-9 instrument at The Ohio State University employing NaCl cells of 0.1-mm thickness.

Magnetic Susceptibilities. The magnetic susceptibility of [*n*-$Bu_4N]_3[Os(CN)_6]$ was measured at The Ohio State University on an apparatus employing the Faraday method. Corrections for diamagnetic atoms were applied in the calculation of μ_{eff}.

Gaussian Analysis. Electronic spectra were analyzed by fitting the observed envelopes to sums of Gaussian curves where absorbance is expressed as a function of wave number. This was accomplished by replotting all points as functions of wave number, estimating the parameters for the transition(s) visually deduced to be the least overlapped by other bands, constructing the curves involved, and subtracting out the absorbance. The resulting difference curves were then used to find appropriate Gaussian half-width, amplitude, and peak location for the remaining transitions. Whenever possible, this procedure was commenced with the highest energy band and continued to the lowest subtracting out peaks one by one. In a few cases, the tails of intense bands peaking >50,000 cm^{-1} were estimated.

Finally, the estimated parameters were input in a Fortran program using Leverberg's[26] method of damped least squares to secure the best fit to the experimental envelope. The fit of almost all points is good to about 4%.

Results

Hexacyanide Molecular Orbitals. The calculation of molecular orbitals iterated to self-consistent charge and configuration (SCCC) for the model complexes ferrocyanide and cobalticyanide has been discussed by us elsewhere.[27a] This same procedure was followed

(23) O. T. Christiansen, *J. Prakt. Chem.*, **31**, 163 (1885).

(24) (a) J. Locke and G. H. Edwards, *Am. Chem. J.*, **20**, 594 (1898); (b) L. Meiter, *J. Am. Chem. Soc.*, **79**, 4631 (1957).

(25) (a) P. T. Manoharan, Ph.D. Thesis, Columbia University, 1965; (b) P. T. Manoharan and H. B. Gray, *Inorg. Chem.*, **5**, 823 (1966).

(26) K. O. Leverberg, *Quart. Appl. Math.*, **2**, 258 (1944).

(27) (a) J. J. Alexander and H. B. Gray, *Coord. Chem. Rev.*, 2, 29 (1967). (b) Ligand wave functions, eigenvectors, and eigenvalues have been deposited as Document No. 9876 with the ADI Auxiliary Publications Project, Photoduplication Service, Library of Congress, Washington 25, D. C. Copies may be secured by citing the document number and remitting in advance $2.50 for photoprints or $1.25 for 35-mm microfilm, payable to Chief, Photoduplication Service, Library of Congress.

Table I. Selected Results of Molecular Orbital Calculations of Metal Hexacyanides[a]

	$Ti(CN)_6^{3-}$	$V(CN)_6^{3-}$	$Cr(CN)_6^{3-}$	$Mn(CN)_6^{3-}$	$Fe(CN)_6^{3-}$	$Co(CN)_6^{3-}$	$Mn(CN)_6^{4-}$	$Fe(CN)_6^{4-}$
				I. Metal H_{ii}				
d	−94.0	−99.8	−103.4	−106.5	−109.7	−112.1	−101.7	−104.3
s	−81.9	−83.2	−83.9	−84.8	−86.6	−86.2	−82.2	−83.5
p	−45.5	−51.2	−48.9	−48.9	−48.5	−47.5	−47.0	−46.3
				II. Ligand H_{ii}[b] (corrected values in parentheses)				
$\sigma_1(a_{1g})$, −129.0 (−139.4); $\sigma_1(e_g)$, −129.0 (−122.5); $\sigma_1(t_{1u})$, −129.0 (−127.9); $\sigma_2(a_{1g})$, −104.0 (−112.0); $\sigma_2(e_g)$, −104.0 (−99.5); $\sigma_2(t_{1u})$, −104.0 (103.4); $\pi(t_{1g})$, −113.0 (−105.9); $\pi(t_{2g})$, −113.0 (−123.3); $\pi(t_{1u})$, −113.0 (−115.9); $\pi(t_{2u})$, −113.0 (−106.7); $\pi^*(t_{1g})$, −40.0 (−35.4); $\pi^*(t_{1u})$, −40.0 (−41.7); $\pi^*(t_{2g})$, −40.0 (−46.5); $\pi^*(t_{2u})$, −40.0 (−36.3).								
				III. Group Overlaps G_{ij}				
A_{1g}								
$G(4s, \sigma_1)$	−0.6249	−0.6590	−0.6875	−0.7112	−0.7299	−0.7445	−0.7112	−0.7299
$G(4s, \sigma_2)$	+0.4353	0.4691	0.5004	0.5289	0.5546	0.5779	0.5289	0.5546
$G(\sigma_1, \sigma_2)$	−0.3047	−0.3047	−0.3047	−0.3047	−0.3047	−0.3047	−0.3047	−0.3047
E_g								
$G(3d, \sigma_1)$	−0.4476	−0.4162	−0.3812	−0.3466	−0.3130	−0.2822	−0.3466	−0.3130
$G(3d, \sigma_2)$	0.2840	0.2805	0.2718	0.2588	0.2439	0.2281	0.2588	0.2439
$G(\sigma_1, \sigma_2)$	0.1112	0.1112	0.1112	0.1112	0.1112	0.1112	0.1112	0.1112
T_{1g}								
$G(\pi, \pi^*)$	0.1226	0.1226	0.1226	0.1226	0.1226	0.1226	0.1226	0.1226
T_{2g}								
$G(3d, \pi)$	0.3149	0.2711	0.2324	0.1994	0.1712	0.1475	0.1994	0.1712
$G(3d, \pi^*)$	−0.3914	−0.3498	−0.3094	−0.2729	−0.2398	−0.2107	−0.2729	−0.2398
$G(\pi, \pi^*)$	−0.0522	−0.0522	−0.0522	−0.0522	−0.0522	−0.0522	−0.0522	−0.0522
T_{1u}								
$G(4p, \sigma_1)$	−0.1138	−0.1268	−0.1442	−0.1611	−0.1727	−0.2047	−0.1611	−0.1727
$G(4p, \sigma_2)$	0.1125	0.1182	0.1244	0.1303	0.1346	0.1451	0.1303	0.1346
$G(4p, \pi)$	0.3564	0.3609	0.3668	0.3722	0.3756	0.3843	0.3722	0.3756
$G(4p, \pi^*)$	−0.2711	−0.2786	−0.2886	−0.2980	−0.3043	−0.3215	−0.2980	−0.3043
$G(\sigma_1, \sigma_2)$	0.0052	0.0052	0.0052	0.0052	0.0052	0.0052	0.0052	0.0052
$G(\pi, \pi^*)$	−0.0699	−0.0699	−0.0699	−0.0699	−0.0699	−0.0699	−0.0699	−0.0699
$G(\sigma_2, \pi)$	−0.0528	−0.0528	−0.0528	−0.0528	−0.0528	−0.0528	−0.0528	−0.0528
$G(\sigma_1, \pi^*)$	0.0756	0.0756	0.0756	0.0756	0.0756	0.0756	0.0756	0.0756
$G(\sigma_2, \pi)$	0.0425	0.0425	0.0425	0.0425	0.0425	0.0425	0.0425	0.0425
$G(\sigma_2 \pi^*)$	−0.0703	−0.0703	−0.0703	−0.0703	−0.0703	−0.0703	−0.0703	−0.0703
T_{2u}								
$G(\pi, \pi^*)$	0.0687	0.0687	0.0687	0.0687	0.0687	0.0687	0.0687	0.0687
				IV. F^k Parameters				
F^σ	1.32	1.35	1.40	1.44	1.52	1.54	1.48	1.53
F^π	2.30	2.30	2.30	2.30	2.30	2.30	2.30	2.30
				V. Metal Charge				
	+0.66	+0.56	+0.47	+0.48	+0.45	+0.41	+0.46	+0.42
				VI. Metal Population				
d	2.85	3.81	4.81	5.95	6.96	8.00	6.02	7.05
s	0.01	0.00	0.01	0.04	0.07	0.09	0.02	0.06
p	0.48	0.63	0.71	0.53	0.52	0.50	0.50	0.47
				VII. Ligand Population				
σ_1	2.02	1.99	1.94	1.93	1.91	1.89	1.96	1.94
σ_2	1.83	1.80	1.76	1.74	1.71	1.67	1.76	1.73
π	1.83	1.87	1.86	1.88	1.93	1.96	1.93	1.97
π^*	0.05	0.07	0.07	0.06	0.05	0.04	0.07	0.06
				VIII. Selected Eigenvalues				
$2t_{1u}$	−117.95	−118.95	−118.89	−118.41	−118.25	−117.50	−118.12	−117.90
$1t_{2u}$	−107.05	−107.05	−107.05	−107.05	−107.05	−107.05	−107.05	−107.05
$1t_{1g}$	−106.89	−106.89	−106.89	−106.89	−106.89	−106.89	−106.89	−106.89
$2a_{1g}$	−105.54	−105.85	−103.55	−104.23	−102.66	−104.26	−104.25	−102.28
$2e_g$	−103.94	−104.51	−107.38	−108.18	−109.63	−109.84	−107.07	−108.48
$3t_{1u}$	−102.11	−102.15	−102.20	−101.79	−101.67	−100.56	−101.77	−101.62
$2t_{2g}$	−70.78	−75.88	−80.77	−85.67	−90.63	−94.23	−83.46	−87.96
$3e_g$	−48.44	−52.48	−54.13	−51.37	−55.68	−59.34	−50.08	−53.42
$4t_{1u}$	−41.11	−42.11	−47.89	−41.57	−41.43	−40.98	−41.25	−41.07
$2t_{2u}$	−34.96	−34.96	−34.96	−34.96	−34.96	−34.96	−34.96	−34.96

[a] All energies in 1000 cm^{-1}. For complete results see ref 27b. [b] Ligand H_{ii}'s are the same for all complexes listed.

for the other hexacyano complexes of first-row transition metals.[27b] A summary of the relevant results is given in Table I. We note that the metal–carbon distance was in all cases taken as 1.89 Å. Figure 1 shows the calculated energy levels for $Fe(CN)_6^{4-}$; a similar ordering of one-electron levels was obtained for all other species treated (namely Ti(III), V(III), Cr(III), Mn(II), Mn(III), Fe(III), and Co(III)) with the exception that scrambling sometimes occurred among sets of levels whose order is not specified on a vertical scale, for example, $2t_{2u}$, $2t_{1g}$, and $3t_{2g}$. In every case, however, the ordering $2t_{2g} < 3e_g < 4t_{1u}$ was obtained for the group

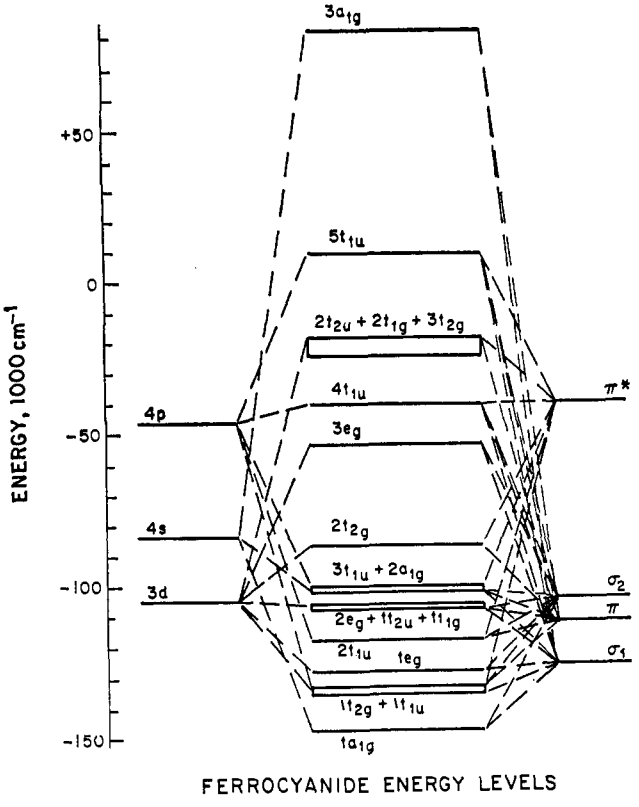

Figure 1. Energy levels of ferrocyanide ion.

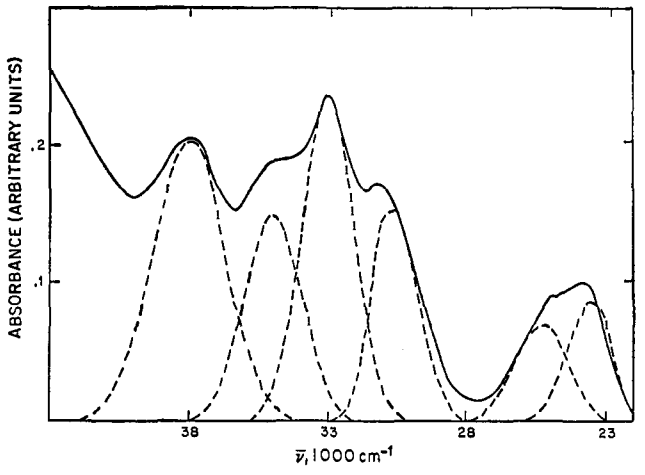

Figure 2a. Electronic spectrum of $[n\text{-}Bu_4N]_3[Fe(CN)_6]$ in EPA at 300°K; (- - -) resolution into Gaussian curves.

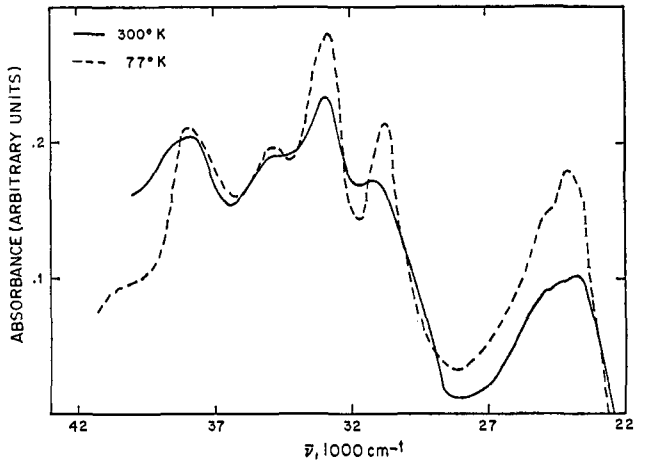

Figure 2b. Electronic spectrum of $[n\text{-}Bu_4N]_3[Fe(CN)_6]$ in EPA (———) at 300°K; (- - -) at 77°K.

levels of importance (*inter alia*) in the electronic transitions.

Every level scheme is filled through the $3t_{1u}$ (or $2a_{1g}$, whichever is higher) by the valence electrons of the six cyanide ligands leaving the metal d electrons to be accommodated in the $2t_{2g}$ level.

Electronic Spectra. Table II presents the observed maxima for hexacyanides in solutions and mulls of their potassium salts, together with extinction coefficients.

d^6 Complexes. We recall[21] that for this configuration of the central metal ion, the $2t_{2g}$ orbital is exactly filled to give a $^1A_{1g}$ ground state. The anticipated d → d excitations are then $^1A_{1g} \rightarrow {}^3T_{1g}$, $^1A_{1g} \rightarrow {}^1T_{1g}$, $^1A_{1g} \rightarrow {}^3T_{2g}$, and $^1A_{1g} \rightarrow {}^1T_{2g}$ arising from the $2t_{2g} \rightarrow 3e_g$ transition; the M → L charge transfers $2t_{2g} \rightarrow 4t_{1u}(^1A_{1g} \rightarrow c^1T_{1u})$ and $2t_{2g} \rightarrow 2t_{2u}(^1A_{1g} \rightarrow d^1T_{1u})$ are also expected to fall potentially in the region of interest (<52,000 cm^{-1}). The spectra of the Fe(II), Ru(II), Os(II), and Co(III) species were assigned earlier[9] in accord with these expectations. Our low-temperature measurements (which are reported in Table III along with band positions, oscillator strengths obtained from Gaussian analysis, and assignments) support the aforementioned interpretation for $Fe(CN)_6^{4-}$ and $Co(CN)_6^{3-}$.[28]

d^5 Complexes. Ferricyanide, $Fe(CN)_6^{3-}$. The hole in the $2t_{2g}$ level gives all d^5 complexes the ground-state configuration, $\ldots(3t_{1u})^6(2t_{2g})^5 = {}^2T_{2g}$. The electronic spectrum of ferricyanide consists of intense bands at 24,000, 33,000, and 38,000 cm^{-1}. Two shoulders are seen on the 33,000-cm^{-1} band at 31,250 and 35,700 cm^{-1}; at 77°K, these are resolved into two bands having maxima at 30,670 and 34,850 cm^{-1}, respectively. Moreover, at this lower temperature, the central maximum shifts to *ca.* 32,800 cm^{-1}, and a new shoulder appears at *ca.* 40,000 cm^{-1}. Also, the high-energy side of the 24,100-cm^{-1} peak becomes slightly more asymmetric. An intense shoulder at 44,500 cm^{-1} and a peak at 50,000 cm^{-1} complete the spectrum. Figure 2 shows spectra in EPA.

We first note that in the d^6 ferrocyanide ion, the M → L charge transfer occurs at >43,000 cm^{-1}, and no other charge-transfer bands are observed. Consequently, any charge transfer seen below this energy in d^5 ferricyanide can safely be attributed to an L → M process. Also, since the final state of the metal ion is $d^6 \equiv {}^1A_{1g}$ (formally), no multiplet structure of these bands is expected. At first glance, it would seem that all bands observed must be parity-allowed g → u on account of their high intensities; however, the two shoulders at *ca.* 31,250 and 35,700 cm^{-1}, as well as the new shoulder at ~40,000 cm^{-1} which appears at low temperature, are

(28) We also note our measurements of the electronic spectrum of $H_4Fe(CN)_6$; this compound was used (since preparation of a tetraalkylammonium salt of ferrocyanide could not be accomplished) to study the temperature dependence of the transitions. The protonation of the nitrogen end of cyanide is evidenced in ethanol by the shift of the first d → d transition from 31,000 to 32,800 cm^{-1} and the M → L charge transfer by some 1600 cm^{-1} to the blue. This indicates increased back-bonding in the protonated species resulting from stabilization of the t_{2g} level; a similar effect is known[28b] with adducts of Lewis acids: D. F. Shriver and J. Posner, *J. Am. Chem. Soc.*, **88**, 1672 (1966).

Table II. Observed Electronic Spectra of Metal Hexacyanide Complexes at 300°K[a]

Complex	Obsd max, cm^{-1} (ϵ)	Complex	Obsd max, cm^{-1} (ϵ)
$K_3V(CN)_6 \cdot 3H_2O$	14,600 (0.05)	$K_4Fe(CN)_6 \cdot 3H_2O$	23,700 (4.7)
	21,500 (37)		31,000 (302)
	28,500 (50)		37,040 (sh ~1000)
	>30,000		45,870 (24,200)
			50,000 (23,700)
$K_3V(CN)_6 \cdot 3H_2O$[b]	23,000		
	28,250	$K_4Ru(CN)_6$[d]	31,000
			48,500
$K_3Cr(CN)_6$	18,870 (sh 0.4)		52,000
	26,500 (90)		
	32,400 (65)	$[n\text{-}Bu_4N]_3[Os(CN)_6]$[c]	24,300 (1450)
	38,000 (6240)		30,150 (1680)
	>50,000		32,600 (2360)
			35,700 (2060)
$K_3Mn(CN)_6$	21,000 (4)		37,900 (sh 1230)
	30,800 (2980)		>50,000
	37,200 (1680)		
	40,200 (sh 3540)	$K_4Os(CN)_6$	47,000 (47,400)
	42,200 (sh 4110)		52,000 (42,900)
	>50,000		
		$K_3Co(CN)_6$	32,100 (243)
$K_4Mn(CN)_6 \cdot 3H_2O$	27,470 (sh 1300)		38,500 (180)
	31,650 (sh 8710)		50,600 (35,400)
	39,525 (31,100)		
	48,100 (53,300)	$K_3Rh(CN)_6$	52,000 (sh 9780)
$K_4Mn(CN)_6 \cdot 3H_2O$[b]	27,470		>52,000
	32,200		
	36,600	$K_3Ir(CN)_6$	>52,000
$K_3Fe(CN)_6$	23,800 (1100)		
	31,200 (sh 1210)		
	33,200 (1549)		
	35,000 (sh 1350)		
	38,400 (1345)		
	45,500 (sh 5480)		
	50,000 (~10,800)		

[a] Solvent is water unless otherwise noted. [b] Nujol mull. [c] Ethanol solution. [d] From ref 9.

likely candidates for assignment as d → d transitions which can "steal" appreciable intensity as a result of their proximity to intense parity-allowed bands. If this be the case, one would anticipate a lessening of their total oscillator strengths at low temperatures.[29] The decline in oscillator strength at 77°K suggests that the 31,250-cm^{-1} transition is d → d as is the one at 35,700 cm^{-1}. The most reasonable assignment seems to be the spin-allowed, almost degenerate pair $^2T_{2g} \rightarrow (^2T_{1g}, {}^2A_{2g})$ at energy $\Delta - 2B - C$ and $^2T_{2g} \rightarrow {}^2E_g$ at $\Delta + 7B - C$. Naiman[10a] has shown that this assignment leads to the values of $\Delta = 34{,}950$, $B = 720$, and $C = 3286$ cm^{-1} for the ligand-field parameters of this ion. The next spin-allowed d → d transition is the $^2T_{2g} \rightarrow (^2T_{1g}, {}^2T_{2g})$ predicted at 41,300 cm^{-1}. This we assign as the 40,000-cm^{-1} shoulder. Since it is not possible to compare the oscillator strength of this band at two temperatures, we offer as evidence of our assignment the fact that the apparent intensity of the shoulder must be increased greatly by its position on the tails of two intense allowed bands.

The value of $\Delta = 35{,}000$ cm^{-1} was used as an estimate of the $2t_{2g} - 3e_g$ separation in ferricyanide; this determines the relative positions of various possible charge-transfer bands to which we now turn. The first of these Laporte-allowed transitions is located at 23,500 cm^{-1} and, for reasons stated above, must be of L → M type. It is one component obtained from Gaussian analysis of the intense asymmetric peak centered at 24,100 cm^{-1}. The other is a weak band at 25,300 cm^{-1} which will be discussed presently. The 23,500-cm^{-1} transition has been the subject of an extended controversy[10,11] as to the nature of the lower level involved in the excitation. The oscillator strength of the band in EPA increases a little at low temperatures (it remains the same in crystalline $K_3Fe(CN)_6$)[11] indicating that the transition is of g → u type. Our calculation is definite in predicting that the electron is excited from the $3t_{1u}$ into the $2t_{2g}$ level.

Transitions to the $3e_g$ level can be ruled out since the lowest such excitation would be predicted to occur at ~11,000 + Δ = 46,000 cm^{-1}, subject to interelectronic-repulsion correction. Further, our assignment is supported by magnetic optical rotary dispersion (MORD) experiments[12] which have recently indicated the excited state in this transition to be of T_{1u} symmetry. Since the $3t_{1u}$ level is predicted[27] to have ~88.7% ligand σ character, our calculation establishes the nature of the process as $t_{1u}\sigma \rightarrow t_{2g}\pi$. Also, the slightly lower intensity of this charge transfer compared to the others in ferricyanide is appropriate[30] for a ($\sigma \rightarrow \pi$)-type excitation.

The second component of the observed band is a weak transition at 25,300 cm^{-1} which is indicated by Gaussian analysis to decrease in intensity at lower temperature. (The analysis is actually not entirely satisfactory since no clear-cut choice is possible among several relative placements and intensities which would fit the observed envelope at room temperature.) In

(29) A. D. Liehr and C. J. Ballhausen, *Phys. Rev.*, **106**, 1161 (1957).

(30) C. K. Jørgensen, "Absorption Spectra and Chemical Bonding in Complexes," Addison-Wesley Publishing Co., Reading, Mass., 1962.

any case, the envelope can only be analyzed into a sum of two Gaussian curves to give a very intense and a very weak band. This low-intensity band which is Laporte-forbidden may be due either to the $^2T_{2g} \rightarrow {}^4T_{2g}$ transition which our choice of ligand-field parameters places at 23,200 cm^{-1} or to the $a_{1g}\sigma \rightarrow t_{2g}\pi$ $^2T_{2g} \rightarrow {}^2A_{1g}$ charge transfer which our calculation predicts to be degenerate with the allowed $t_{1g}\sigma \rightarrow t_{2g}\pi$. The experiments do not distinguish between the two possibilities; however, we are inclined toward the latter choice since it seems doubtful that a transition which is both spin- and parity-forbidden could "steal" the observed intensity.

The presence of the weak 25,300-cm^{-1} band is important in explaining the high-energy shoulder which begins to appear[31] on the asymmetric band with increasing pressure. The d → d band would surely increase in energy with pressure, while the $a_{1g}\sigma \rightarrow t_{2g}\pi$ band might or might not depending upon the actual reduction in the physical dimensions of the complex and the attendant effect on the $4s\text{-}\sigma_{CN}$ interaction. Nevertheless, the mechanism of intensity decrease with pressure increase observed by Parsons and Drickamer[31] remains obscure.

Remaining charge transfers to be accounted for are those at 33,000, 38,460, and 44,000 cm^{-1}. The calculated energy level scheme predicts the $t_{2u}\pi \rightarrow t_{2g}\pi$ to be at 31,000 cm^{-1} and the $t_{1g}\pi \rightarrow t_{2u}\pi$ to be ~15,200 cm^{-1} above the first band. Thus, we confidently assign these as the observed bands 33,000 ($t_{2u}\pi \rightarrow t_{2g}\pi$) and 38,460 cm^{-1} ($t_{1u}\pi \rightarrow t_{2g}\pi$). Again, these assignments are confirmed by the constancy of their oscillator strengths at liquid nitrogen temperature and by MORD measurements.[12] The first M → L band is calculated at 43,200 cm^{-1} and therefore must be associated with the one observed at 44,000 cm^{-1}; it is the excitation $2t_{2g}\pi \rightarrow 4t_{1u}\pi^*$. The final intense transition at ~50,000 cm^{-1} is assigned as the M → L process $t_{2g}\pi \rightarrow t_{2u}\pi^*$ calculated at ~50,000 cm^{-1}. The bands observed as well as our assignments are summarized in Table III, where the symmetry labels refer to the states involved in the transition.

Manganocyanide, $Mn(CN)_6^{4-}$. The isoelectronic $Mn(CN)_6^{4-}$ ion displays a spectrum containing four bands at 27,470, 31,650, 39,250, and 48,070 cm^{-1} as seen in Figure 3. Although the extreme sensitivity of this complex to oxidation precluded the examination of its spectrum at liquid N_2 temperature, we believe that the reasonably well-separated band profiles are evidence that the last three bands are not d → d transitions which "steal" intensity.

We should expect by reason of the lesser stability of the metal orbitals brought about by the lower atomic number and formal oxidation state of Mn(II) that L → M charge transfer would come at higher energy and M → L charge transfer at lower energy than in $Fe(CN)_6^{3-}$. This prediction is borne out by the calculation which places $t_{1u}\sigma \rightarrow t_{2g}\pi$ at 22,000 cm^{-1}, $t_{2u}\pi \rightarrow t_{2g}\pi$ at 28,000 cm^{-1}, and $t_{1u}\pi \rightarrow t_{2g}\pi$ at 40,000 cm^{-1}. Moreover, the M → L bands are predicted at 36,000 cm^{-1} for $t_{2g}\pi \rightarrow t_{1u}\pi^*$ and 42,000 cm^{-1} for $t_{2g}\pi \rightarrow t_{2u}\pi^*$. By reason of its small oscillator strength (~0.0087), we assign the 27,470-cm^{-1} band as the ligand-field band $^2T_{2g} \rightarrow (^2A_{2g}, {}^2T_{1g})$, since the two excited states are practically degenerate. Estimating $\Delta \sim$ 30,000 cm^{-1} and letting $B \simeq 425$ cm^{-1} while $C \sim 4B =$ 1800 cm^{-1}, the other spin-allowed bands would be expected to fall under the intense charge transfers which follow. The first intense transition at 31,650 cm^{-1} is the $t_{1u}\sigma \rightarrow t_{2g}\pi$ excitation, placed at higher energy than Fe(III) as would be expected.

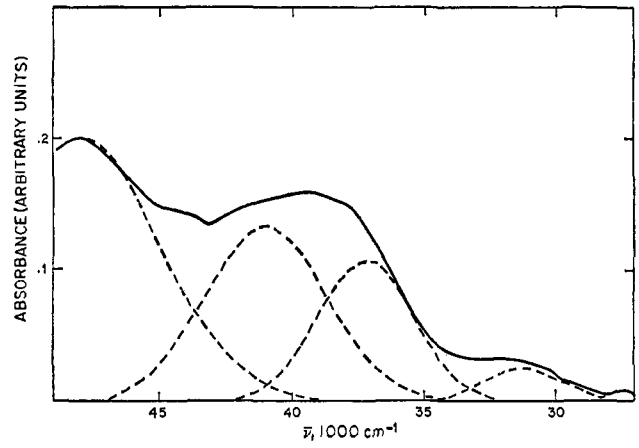

Figure 3. Electronic spectrum of $K_4Mn(CN)_6$ in 1.5 *M* aqueous KCN; (- - -) resolution into Gaussian curves.

Gaussian analysis reveals that the experimentally observed envelope centered at 39,500 cm^{-1} contains two transitions of about the same intensity at 41,000 and 37,200 cm^{-1}. The fact that both M → L and L → M charge transfers are calculated to appear in an overlapping spectral region for manganocyanide makes the transitions difficult to sort out by experimental means except for MORD determinations of excited-state symmetries. We note in going from Co(III) to Fe(II), where the configuration is the same and the atomic number and oxidation state differ by one unit, that the position of the $t_{2g}\pi \rightarrow t_{1u}\pi^*$ transition moves from 49,500 to 45,900 cm^{-1}; using this as a rough estimate of the same effect in isoelectronic d^5 complexes, the M → L band $2t_{2g}\pi \rightarrow 3t_{1u}\pi^*$ would be placed around 40,500 cm^{-1}, and so the peak at 41,000 cm^{-1} is ascribed to this excitation. This leaves the band at 37,200 cm^{-1} for assignment as L → M $t_{2u}\pi \rightarrow t_{2g}\pi$ in rather good agreement with its calculated position *vis-á-vis* the first L → M band and exhibiting a separation quite similar to the one in ferricyanide. The $t_{1u}\pi \rightarrow t_{2g}\pi$ excitation (calculated at 40,000 cm^{-1}) probably also appears unresolvably near the band at 41,000 cm^{-1}; thus, the Gaussian envelope is expected to contain two transitions. Finally, the 48,000-cm^{-1} band is assigned as the $2t_{2g} \rightarrow 2t_{2u}\pi^*$ M → L transition, whose energy should be lower than in the ferricyanide case.

Our assignments for $Mn(CN)_6^{4-}$ are reported in Table III.

Osmicyanide, $Os(CN)_6^{3-}$. The hexacyano complex of Os(III) which was here isolated for the first time has a spectrum quite like that of its first-row analog ferricyanide. Its μ_{eff} of 2.12 BM at 296°K is consistent with a single unpaired electron. The spectrum of $Os(CN)_6^{3-}$ is shown in Figure 4. A very broad band (compared with the lowest energy transition in $Fe(CN)_6^{3-}$) is centered around 24,000 cm^{-1}; this is followed by a less intense broad shoulder which seems

(31) R. W. Parsons and H. G. Drickamer, *J. Chem. Phys.*, **29**, 930 (1958).

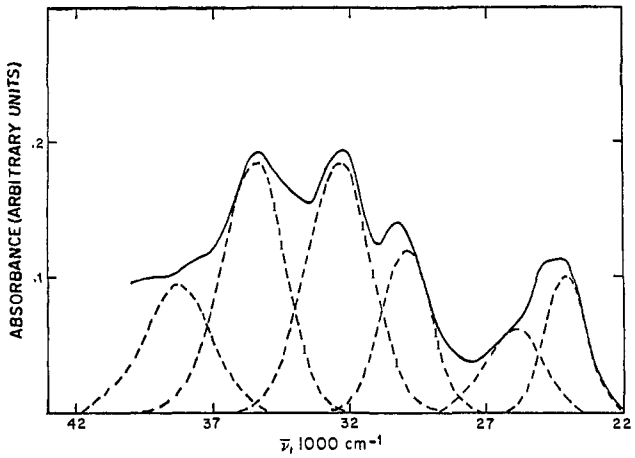

Figure 4a. Electronic spectrum of $[n\text{-Bu}_4\text{N}]_3[\text{Os(CN)}_6]$ in EPA at 300°K; (- - -) resolution into Gaussian curves.

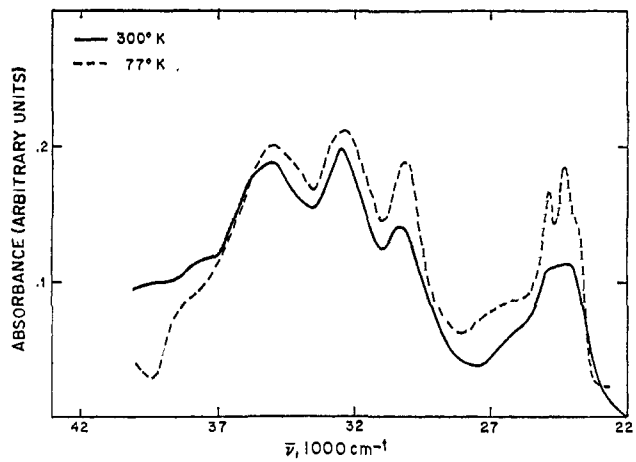

Figure 4b. Electronic spectrum of $[n\text{-Bu}_4\text{N}]_3[\text{Os(CN)}_6]$ in EPA (———) at 300°K; (- - -) at 77°K.

to peak at *ca.* 27,000 cm^{-1}. The central group of three transitions is again present, this time with maxima at 29,900, 32,400, and 35,400 cm^{-1}. A shoulder on the last band at 38,300 cm^{-1} is followed by slowly rising absorption. On cooling, this spectrum reveals several interesting features. The low-energy broad band splits into two quite narrow components at 24,200 and 25,050 cm^{-1}, the half-width of the first being only ~600 cm^{-1}. Comparison of the sum of the oscillator strengths of these narrow peaks with that of the broad one seen at 300°K shows a considerable increase (~1.4 times) in intensity at the lower temperature. The transition at 27,000 cm^{-1} appears to retain its intensity as well, but, when corrected for the intensity increase in the neighboring band, it is seen to decrease by about one-third. It must be Laporte-forbidden then.

Oscillator strengths of the maxima at 29,900 and 32,400 cm^{-1} increase while those at 35,400 cm^{-1} and its shoulder decrease. Obviously, this last group of bands is just the pattern observed in Fe(CN)_6^{3-} with the ligand-field transitions shifted to higher energy than the charge transfers.

The d → d bands at 35,400 and 38,300 cm^{-1} are assigned as the first two spin-allowed excitations because (a) their intensities make a doublet → quartet process improbable; (b) this yields the expected increase in Δ and decrease in B for a third-row complex over first row. Thus, we have $^2T_{2g} \rightarrow (^2A_{1g}, {}^2T_{2g})$ at 35,400 cm^{-1} and $^2T_{2g} \rightarrow {}^2E_g$ at 38,300 cm^{-1}. This leads to a $\Delta \sim 38{,}000$ cm^{-1}, $B \sim 340$ cm^{-1}, and $C \sim 1700$ cm^{-1}. Such a choice of ligand-field parameters places the other d → d bands as follows.

$^2T_{2g} \rightarrow {}^4T_{2g}$	29,500 cm^{-1}
$\rightarrow {}^4T_{1g}$	32,300 cm^{-1}
$\rightarrow {}^2T_{1g}(2)$	42,000 cm^{-1}
$\rightarrow {}^2T_{2g}(2)$	46,600 cm^{-1}
$\rightarrow {}^6A_{1g}$	54,000 cm^{-1}

These transitions are placed under charge-transfer bands and are not observed.

Moving to a consideration of the charge transfers, we expect that no M → L excitations should be seen at <48,000 cm^{-1} for reasons analogous to the d^5 ferricyanide case. We have four peaks which retain intensity at low temperature and only three allowed processes for the low-energy L → M charge transfer. The first two narrow peaks (which are unresolved at room temperature) are assigned as components of the $t_{1u}\sigma \rightarrow t_{2g}\pi$ excitation split by the spin-orbit coupling of the Os 6p orbital. Under intermediate coupling, the $^2T_{2g}$ ground state splits into E_g'' (at $-\xi_{5d}$) and U_g' (at $+\frac{1}{2}\xi_{5d}$). Since only E_g'' is expected to be populated at 77°K, our assignment requires the resolution into Kramers doublets of the U_u' state arising[32] from the excited state a^2T_{1u}; this is because the transition $E_g'' \rightarrow E_u'$ is forbidden (E_u' is the other component of a^2T_{1u}). The observation of the two bands separated by approximately 850 cm^{-1} is probably due to a low-symmetry ligand field brought about by ion pairing of Os(CN)_6^{3-} with $n\text{-Bu}_4\text{N}^+$ cations in the rigid glass.

The bands at 32,400 and 35,400 cm^{-1} do not show the structure of the first band system. By analogy with ferricyanide, these bands are assigned to the $t_{2u}\pi \rightarrow t_{2g}\pi$ and $t_{1u}\pi \rightarrow t_{2g}\pi$ transitions, respectively.

We are left with the broad parity-forbidden band at 27,000 cm^{-1}. This must be a forbidden $L_g \rightarrow t_{2g}\pi$ charge transfer; supposing that the level scheme remains the same from the first row, it must be $a_{1g}\sigma \rightarrow t_{2g}\pi$ ($^2T_{2g} \rightarrow {}^2A_{1g}$). There seems to be no good reason for assigning it in any other way, particularly since designation as a d → d excitation would require it to be spin allowed and lead to $\Delta(\text{Os}) < \Delta(\text{Fe})$ as well as unsatisfying values of *B* and *C*.

The fact that a third-row hexacyano complex displays charge transfers at the same (or slightly lower) energy than isoelectronic first-row species is rather surprising in light of the anticipated decrease in metal orbital stability and will be discussed presently.

The striking similarity of the three-band system in ferricyanide and osmicyanide, as well as the fact that the band separations are around the value of the cyanide stretching frequency, might be regarded as evidence that the two side bands are in fact vibrational components of the main transition. On closer examination, this argument appears a good deal less attractive. The separation between the second and third bands of the series is 2000 cm^{-1} in the Fe(III) complex and 2900 cm^{-1} in the Os(III), while the first and second bands are 2300 and 2500 cm^{-1} apart, respectively. Except for

(32) C. K. Jørgensen, *Mol. Phys.*, 2, 309 (1959).

Table III. Metal Hexacyanide Spectra with Intensity Analysis at Room and Low Temperatures

Complex	Solvent	Band, cm^{-1} [a]	$\epsilon \times 10^{-2}$ [a]	$P \times 10^{-2}$ [a]	Low-temp technique	Behavior at low temp[b]	Assignment[a]
$K_3Ti(CN)_6$	Liq NH_3	18,900				Not obsd	$^2T_{2g} \rightarrow {}^2E_g$
		22,300				Not obsd	
$K_3V(CN)_6$	H_2O	14,600	0.0521	~0.0006	None	Not obsd	$^3T_{1g} \rightarrow {}^1T_{2g}$
		19,200	0.0702	0.001		Not obsd	$^3T_{1g} \rightarrow {}^1T_{1g}$
		22,700	0.427	0.094		Not obsd	$^3T_{1g} \rightarrow {}^3T_{2g}$
		27,200	~0.600	~0.132		Not obsd	$^3T_{1g} \rightarrow {}^3T_{1g}$
		>30,000					
$K_3Cr(CN)_6$	H_2O	18,500	0.004	0.0038	*d*		$^4A_{2g} \rightarrow {}^2T_{2g}$
		26,600	0.803	0.148		Decreases	$^4A_{2g} \rightarrow {}^4T_{2g}$
		32,500	0.613	0.116		Decreases	$^4A_{2g} \rightarrow {}^4T_{1g}$
		38,600	59.4	9.78		Increases	$^4A_{2g} \rightarrow {}^4T_{2u}$
		>50,000					
$K_3Mn(CN)_6$	H_2O	21,000	0.0398	0.0033	*d*	Decreases	$^3T_{1g} \rightarrow ({}^1E_g, {}^1T_{2g})$
		31,100	36.7	4.56		Same	$^3T_{1g} \rightarrow {}^3T_{2u}$
		33,150	10.98	0.755		Decreases?	$^3T_{1g} \rightarrow {}^3A_{1g}$
		36,700	11.70	1.613		Decreases?	$^3T_{1g} \rightarrow {}^3T_{1u}$
		41,100	16.21	2.38		Decreases?	$^3T_{1g} \rightarrow {}^3T_{2u}$
		>50,000					
$K_4Mn(CN)_6$	H_2O	27,400	5.92	0.708	None	Not obsd	$^2T_{2g} \rightarrow ({}^2T_{1g}, {}^2A_{2g})$
		31,250	26.5	3.17		Not obsd	$^2T_{2g} \rightarrow a\,{}^2T_{1u}$
		37,200	121.0	14.47		Not obsd	$^2T_{2g} \rightarrow a\,{}^2T_{2u}$
		41,000	150.5	18.00		Not obsd	$^2T_{2g} \rightarrow b\,{}^2T_{1u}$ $^2T_{2g} \rightarrow c\,{}^2T_{1u}$
		48,000	227.0	22.1		Not obsd	$^2T_{2g} \rightarrow d\,{}^2T_{1u}$
$[n\text{-}Bu_4N]_3[Fe(CN)_6]$	EPA	23,500	4.93	0.408	*c*	Same	$^2T_{2g} \rightarrow a\,{}^2T_{1u}$
		25,300	3.95	0.400		Decreases	$^2T_{2g} \rightarrow {}^2A_{1g}$
		30,700	8.76	0.725		Decreases	$^2T_{2g} \rightarrow ({}^2T_{1g}, {}^2A_{2g})$
		33,000	13.38	1.355		Same	$^2T_{2g} \rightarrow a\,{}^2T_{2u}$
		35,000	8.64	0.944		Decreases	$^2T_{2g} \rightarrow {}^2E_g$
		38,460	11.57	2.165		Same	$^2T_{2g} \rightarrow b\,{}^2T_{1u}$
		44,000	54.8			Not obsd	$^2T_{2g} \rightarrow c\,{}^2T_{1u}$
		50,000	107.8	39.4		Not obsd	$^2T_{2g} \rightarrow d\,{}^2T_{1u}$
$[n\text{-}Bu_4N]_3[Os(CN)_6]$	EPA	24,100	9.52	0.788	*c*	Increases	$^2T_{2g} \rightarrow a\,{}^2T_{1u}$
		26,000	4.13	0.475		Decreases	$^2T_{2g} \rightarrow {}^2A_{1g}$
		29.900	11.41	1.076		Increases	$^2T_{2g} \rightarrow a\,{}^2T_{2u}$
		32,400	12.18	1.51		Increases	$^2T_{2g} \rightarrow b\,{}^2T_{1u}$
		35,400	12.25	1.52		Decreases	$^2T_{2g} \rightarrow ({}^2T_{1g}, {}^2A_{2g})$
		38,300	6.26	0.806		Decreases	$^2T_{2g} \rightarrow {}^2E_g$
		>50,000					
$K_4Os(CN)_6$	H_2O	47,950	493.0	143.0	None	Not obsd	$^1A_{1g} \rightarrow c\,{}^1T_{1u}$
		51,300	~250			Not obsd	$^1A_{1g} \rightarrow d\,{}^1T_{1u}$
$[n\text{-}Bu_4N]_3[Co(CN)_6]$	EPA	31,800	1.385	0.280	*c*	Decreases	$^1A_{1g} \rightarrow {}^1T_{1g}$
		38,700	1.09	0.241		Decreases	$^1A_{1g} \rightarrow {}^1T_{2g}$
		49,500	229.0	63.1		Not obsd	$^1A_{1g} \rightarrow c\,{}^1T_{1u}$
$K_3Rh(CN)_6$	H_2O	52,000	29.2	12.1	None	Not obsd	$^1A_{1g} \rightarrow c\,{}^1T_{1u}$
		>52,000					
$K_3Ir(CN)_6$	H_2O	>52.000			None		
$K_4Fe(CN)_6$	H_2O	23,700	0.047	0.007	*e*	Decreases	$^1A_{1g} \rightarrow {}^3T_{1g}$
		31,000	3.04	0.73		Decreases	$^1A_{1g} \rightarrow {}^1T_{1g}$
		(32,800)[f]	(3.18)				
		37,040[b]		0.47		Decreases?	$^1A_{1g} \rightarrow {}^1T_{2g}$
		45,870	237.0	66.6		Not obsd	$^1A_{1g} \rightarrow c\,{}^1T_{1u}$
		(47,500)[f]	(186.0)				
		50,000		6.37		Not obsd	$^1A_{1g} \rightarrow d\,{}^1T_{1u}$
$K_4Ru(CN)_6$[g]	H_2O	31,000			None	Not obsd	$^1A_{1g} \rightarrow {}^1T_{1g}$
		48,500		85.0		Not obsd	$^1A_{1g} \rightarrow c\,{}^1T_{1u}$
		52,000		45.0		Not obsd	$^1A_{1g} \rightarrow d\,{}^1T_{1u}$

[a] Band positions, extinction coefficients, and oscillator strengths given are those obtained from Gaussian analysis of spectrum of the complex in the solvent specified. In d^5 and d^6: $aT_{1u} = 3t_{1u} \rightarrow 2t_{2g}$; $bT_{1u} = 2t_{1u} \rightarrow 2t_{2g}$; $cT_{1u} = 2t_{2g} \rightarrow 4t_{1u}$; $dT_{1u} = 2t_{2g} \rightarrow 2t_{2u}$; $aT_{2u} = 1t_{2u} \rightarrow 2t_{2g}$. [b] Low-temperature behavior of bands obtained from a comparison of oscillator strengths in the specified low-temperature solvent at both room temperature and that of the glass. [c] Tetraalkylammonium salt in EPA; cooled to 77°K. [d] Potassium salt in 2:1 ethylene glycol–water; cooled to 143°K. [e] $H_4Fe(CN)_6$ in 7:3 isopentane–butanol; cooled to 77°K. [f] $H_4Fe(CN)_6$ in EtOH. [g] From ref 9.

the first, all these separations are considerably in excess of the totally symmetric C–N stretch (which is the vibrational mode whose progressions are to be expected on a Laporte-allowed band). If anything, vibrational structure in the excited state would be expected to exhibit rather lower frequencies than the totally symmetric C–N mode for the ground electronic state. Moreover, the behavior of the first band on freezing to 77°K is different in the two cases.

Manganicyanide, $Mn(CN)_6^{3-}$. The only d^4 member of the series of hexacyanides investigated here is the $Mn(CN)_6^{3-}$ ion. The solution spectrum of manganicyanide (displayed in Figure 5) shows a very weak transition at 21,000 cm^{-1} followed by an intense band peaking at 30,800 cm^{-1}. The 36,700-cm^{-1} excitation is located on the tail of a very broad, strong absorption peaking >50,000 cm^{-1} and displaying shoulders at *ca.* 40,200 and 42,200 cm^{-1}. Resolution of the envelope

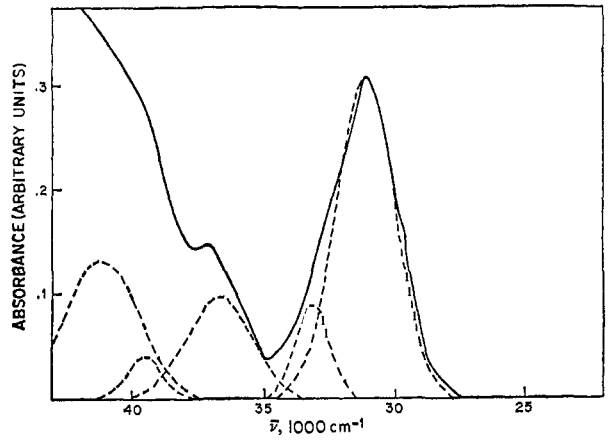

Figure 5a. Electronic spectrum of $K_3Mn(CN)_6$ in 1.5 *M* aqueous KCN; (- - -) resolution into Gaussian curves.

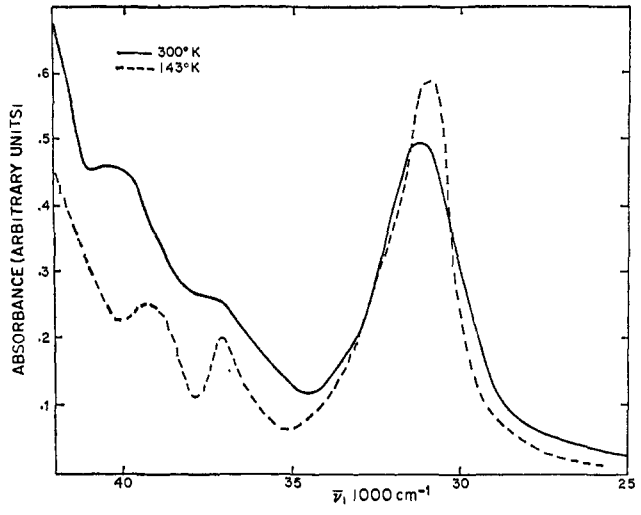

Figure 5b. Electronic spectrum of $K_3Mn(CN)_6$ in 2:1 ethylene glycol-water saturated with KCN; (———) at 300°K; (- - -) at 143°K.

~30,800 cm^{-1} to a sum of Gaussian bands yields an intense transition at 31,100 cm^{-1}, whose oscillator strength does not decrease with a decrease in temperature, and a weaker one at 33,150 cm^{-1}, which does decrease. Estimating the tail of the high-energy band, the resolution shows a narrow, intense transition at 36,700 cm^{-1}, a weak one at 39,500 cm^{-1}, and another high-intensity peak at 41,100 cm^{-1}. The intensities of all three components seem to decrease with temperature, but this could easily be only an apparent effect since the tail of the band where they are located is undoubtedly narrowing. Thus, our experiments do not rigorously establish that the three transitions in question are orbitally forbidden.

By observing one of the red crystals of this complex, Jones and Runciman[33] found a series of very weak lines at ~10,500 cm^{-1} which are not seen in solution.

Dealing first with the low-intensity bands, we note that their weakness establishes them as spin-forbidden; the low-lying states of $(t_{2g})^4$ are[34] (^1E_g, $^1T_{2g}$) and $^1A_{1g}$ at energies $6B + 2C$ and $15B + 5C$. For the choice of assignment 10,500 cm^{-1} as $^3T_{1g} \rightarrow$ (^1E_g, $^1T_{2g}$) and taking B = 660 cm^{-1} and C = 3280 cm^{-1}, we predict $^3T_{2g} \rightarrow {}^1A_{1g}$ at 25,800 cm^{-1}. We associate this transition with the band observed at 21,000 cm^{-1} whose extinction coefficient of ~4 is in line with such an assignment.

Treating the next intense band at 31,100 cm^{-1}, we recall its constant intensity at 77°K establishes it as Laporte-allowed. The calculations predict[27] that the $t_{1u}\sigma \rightarrow t_{2g}\pi$ excitation in $Mn(CN)_6^{3-}$ should come at ~6000 cm^{-1} higher energy than in ferricyanide and ~1000 cm^{-1} lower than in $Mn(CN)_6^{4-}$. Thus we assign the 31,100-cm^{-1} band as the $t_{1u}\sigma \rightarrow t_{2g}\pi$ transition.

Choosing $\Delta \sim$ 34,000 cm^{-1} slightly lower than $Fe(CN)_6^{3-}$, we can place the $^3T_{1g} \rightarrow {}^3E_g(1)$ transition at 32,000 cm^{-1} and $^3T_{1g} \rightarrow {}^3A_{1g}$ at *ca.* 32,700 cm^{-1}. Either of these could account for the weak parity-forbidden transition obtained from Gaussian analysis at 33,150 cm^{-1}. Other low-lying states of interest would be the $^3T_{1g}$ and $^3E_g(2)$ calculated to fall at 33,360 and 37,316 cm^{-1}, respectively, and $^3T_{2g}(1)$ at 37,960 cm^{-1}; these should all fall under the envelope of the 37,000-cm^{-1} transition, but none is resolved at 77°K. The highest state of interest is the $^3A_{2g}$ at 38,600 cm^{-1}, which could possibly be the band at 39,500 cm^{-1}. However, the observed band coincides with a very strong band in $Mn(CN)_6^{4-}$, making it highly suspect. Hence, we omit it from our table of bands definitely assignable to the $Mn(CN)_6^{3-}$ species.

Alternatively, the weak band at 33,150 cm^{-1} could be due to the $a_{1g}\sigma \rightarrow t_{2g}\pi$ excitation calculated to be ~2000 cm^{-1} above the first L → M band. Again, our experiments do not distinguish.

On the basis of our calculation and admittedly inconclusive intensity data, we feel that the 37,000-cm^{-1} band should be assigned to the $t_{2u}\pi \rightarrow t_{2g}\pi$ L → M charge-transfer transition, which is calculated to fall ~5000 cm^{-1} above $t_{1u}\sigma \rightarrow t_{2g}\pi$. As a rather strong supporting argument, we note that this transition is placed similarly to its analogous bands in $Mn(CN)_6^{4-}$ and $Fe(CN)_6^{3-}$ in relation to the first L → M peaks.

Finally, our calculations here place the M → L $t_{2g}\pi \rightarrow t_{1u}\pi^*$ transitions below the L → M $t_{1u}\pi \rightarrow t_{g2}\pi$. In this case, the calculation suggests that the third band would not be seen before about 47,000 cm^{-1}. We, therefore, ascribe the shoulder at 41,100 cm^{-1} to the M → L process $^3T_{1g} \rightarrow {}^3T_{1u}$. Again, the oscillator strength data are inconclusive for reasons given above. The calculated energy is a reasonably satisfying 35,500 cm^{-1}.

d^3 Complexes. Chromicyanide, $Cr(CN)_6^{3-}$. The spectrum of $Cr(CN)_6^{3-}$ is shown in Figure 6. In aqueous solution bands at 26,600 and 32,500 cm^{-1} are of intensity appropriate for d → d transitions; these bands decrease in intensity at 77°K. An intense peak at 38,600 cm^{-1} retains its oscillator strength at low temperature. The only spin-allowed, one-electron transitions possible from the $\ldots(t_{2g})^3 \equiv {}^4A_{2g}$ ground state are $^4A_{2g} \rightarrow {}^4T_{2g}$ and $^4A_{2g} \rightarrow {}^4T_{1g}$ in order of increasing energy. We associate these with the two observed bands. The first directly gives Δ = 26,600 cm^{-1} and from the second $B \sim$ 485 cm^{-1}. A transition observed in emission[35] places the spin-forbidden

(33) G. D. Jones and W. A. Runciman, *Proc. Phys. Soc.* (London), 76, 996 (1960).
(34) Y. Tanabe and S. Sugano, *J. Phys. Soc. Japan*, 9, 766 (1954).
(35) G. B. Porter and H. L. Schläfer, *Z. Physik. Chem.* (Frankfurt), 40, 280 (1964).

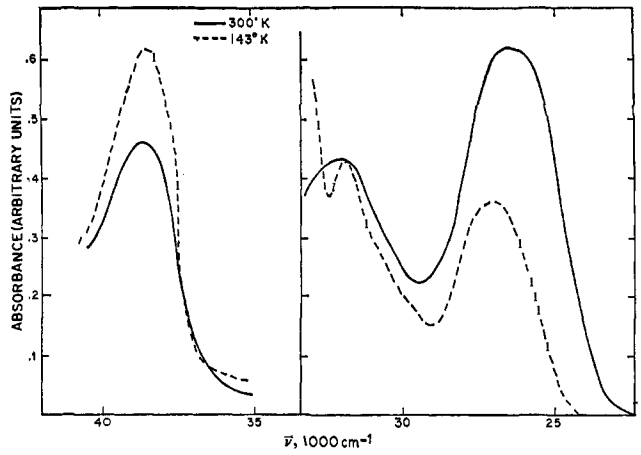

Figure 6. Electronic spectrum of $K_3Cr(CN)_6$ in 2:1 ethylene glycol-water; (———) at 300°K; (- - -) at 143°K.

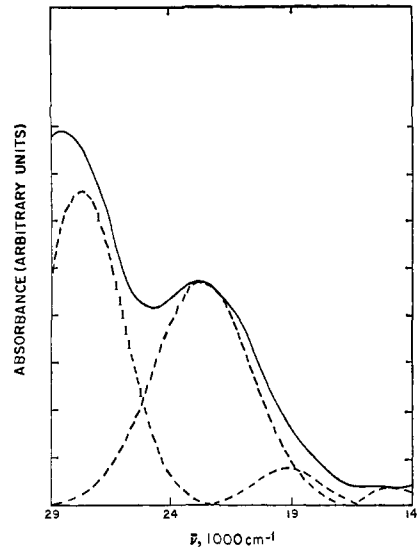

Figure 7. Electronic spectrum of $K_3V(CN)_6$ in 2 *M* aqueous KCN; (- - -) resolution into Gaussian curves.

$^4A_{2g} \rightarrow {}^2E_g$ at 12,820 cm^{-1} and permits evaluation of *C* as 2800 cm^{-1}.

Clearly the absorption at 38,600 cm^{-1} is a charge-transfer transition; the question is whether the process is L → M or M → L. We noted at manganocyanide that the energy of M → L electron transfer was dropping into the region of rising L → M energy. Though the energies of $t_{1u}\sigma \rightarrow t_{2g}\pi$ and $t_{2g}\pi \rightarrow t_{1u}\pi^*$ are calculated to be about the same (even with inclusion of interelectronic repulsion the bands are within 2000 cm^{-1} of each other with the M → L excitation at lower energy, however) and even though simple extrapolation from Fe(III) through Mn(III) would seem to place both processes *ca.* 38,000 cm^{-1}, we attribute the observed band to $t_{2g} \rightarrow t_{1u}\pi^*$. We do this on the ground that no transition is observed at higher energy as would be expected for the other choice. That is to say, if the 38,600-cm^{-1} transition is really L → M, we should anticipate seeing M → L at just slightly greater wave number. Since only a rising absorption is visible, we conclude that the bands have already crossed and that L → M must be 40,000 cm^{-1} or higher. Alternatively, both transitions might be under the 38,000-cm^{-1} peak, but no low-temperature splitting is observed. We consequently reaffirm our attribution of this peak as M → L.

d^2 Complexes. Vanadicyanide, $V(CN)_6^{3-}$. The unstable $V(CN)_6^{3-}$ complex has been investigated in the visible and near-ultraviolet regions where it shows two transitions at 22,700 and 27,700 cm^{-1} whose intensities require that they be spin-allowed ligand-field bands. These two excitations are also visible in a Nujol mull and in diffuse reflectance.[13] In addition, a less intense band is resolved at 14,700 cm^{-1}; this, by reason of its intensity is a spin-forbidden ligand-field transition. The asymmetrical shape of the 22,700-cm^{-1} band indicates another transition under the envelope; Perumareddi, *et al.*,[36] report that this transition is sometimes resolved. In any case, Gaussian analysis places its position at 19,200 cm^{-1}. We have never witnessed the resolution of this band, even though we repeated the measurement several times and obtained agreement of around 7% in our extinction coefficients.

The d → d spectrum observed (Figure 7) is assigned as $^3T_{1g} \rightarrow {}^3T_{2g}$ and $^3T_{1g}(1) \rightarrow {}^3T_{1g}(2)$ for the spin-allowed bands and $^3T_{1g} \rightarrow ({}^1T_{2g}, {}^1E_g)$ and $^3T_{1g} \rightarrow {}^1A_{1g}$. A Δ value of 23,600 cm^{-1} is indicated.

The first charge-transfer sets in at >30,000 cm^{-1}. Although we have not observed its maximum, our calculations indicate that it should possess M → L character and fall at *ca.* 32,000 cm^{-1}.

d^1 Complexes. Titanicyanide, $Ti(CN)_6^{3-}$. We present the spectral results on $Ti(CN)_6^{3-}$ for the sake of completeness. The one observed transition (exhibiting a Jahn-Teller doublet appearance) around 22,300 cm^{-1} is assigned as $^2T_{2g} \rightarrow {}^2E_g$. Both charge transfers are calculated to lie in the 30,000-40,000-cm^{-1} region, but no experimental observations exist in this area. We do, however, expect that the first Laporte-allowed band should be the M → L one and appear at energies lower than the first intense peak in vanadicyanide.

Discussion

Trends in Charge-Transfer Bands. Our assignments and calculations clearly reveal the plausible fact that charge-transfer transitions are determined by the stabilities of metal valence orbitals. The first L → M charge transfer is seen to decrease monotonically from >38,600 to ~24,000 cm^{-1} in going from Cr(III) to Fe(III), paralleling the increase in metal orbital stability with atomic number. Also, the first M → Lπ^* charge transfer goes from a calculated position of ~32,000 cm^{-1} in $Ti(CN)_6^{3-}$ to 53,000 cm^{-1} in $Co(CN)_6^{3-}$; the observed trend is from 38,600 cm^{-1} in Cr(III) to 50,000 cm^{-1} in Co(III). The same observation is valid for M → L processes in an isoelectronic series; thus, we have $2t_{2g} \rightarrow 4t_{1u}$ at 44,000 cm^{-1} in Fe(III) and 41,000 cm^{-1} in Mn(II) as expected from the increase in metal orbital stability with oxidation state and atomic number.

The lower ionization potentials[37] of third-row metals suggest diagonal Hamiltonian matrix elements rather less stable than those of the first row (even allowing for

(36) J. R. Perumareddi, A. D. Liehr, and A. W. Adamson, *J. Am. Chem. Soc.*, **85**, 249 (1963).

(37) C. E. Moore, "Atomic Energy Levels," National Bureau of Standards Circular 467, Vol. I, II, and III, 1949, 1952, 1958, U. S. Government Printing Office, Washington, D. C.

smaller interelectronic repulsions); for the same choice of cyanide orbital energies the position of the first electron-transfer transition should shift to higher energies in the order Fe < Ru < Os. The halides are a nice realization of this expectation; the first L → M peak[30] shifts from 28,650 cm^{-1} in $RuCl_6^{3-}$ to 35,450 cm^{-1} in $OsCl_6^{3-}$, to take one instance. No such clear trend is seen in the cyanides where ferricyanide displays its first L → M band at 23,500 cm^{-1} while in osmicyanide it is at 24,100 cm^{-1}. DeFord and Davidson[38] reported the preparation of solutions which they believed to contain $Ru(CN)_6^{3-}$ and having a spectrum like those for Fe(III) and Os(III) which showed (*inter alia*) a broad band at ~24,200 cm^{-1}; this band must also represent the transition under discussion. The constant L → M energy is evidence of a surprisingly constant orbital electronegativity of the metal t_{2g} going down the iron group. We emphasize again that reduction in interelectronic repulsion effects would compensate for part of the anticipated energy increase since $B(Os) \sim {}^1/_2 B(Fe)$; still, though, we are left with a shift of at least 3000 cm^{-1} (estimated from Jorgensen's orbital electronegativities[39]) which is expected but not seen.

This relative independence of the $t_{1u}\sigma \rightarrow t_{2g}\pi$ transition from atomic number (in spite of the decreasing stability of the metal diagonal matrix element of energy) represents a considerable lowering of the $2t_{2g}\pi$ energy with respect to the ligand based $3t_{1u}$ level. Such an effect is compatible with increased M → π^* bonding. We offer as evidence of this effect the CN stretching frequencies of 2105 cm^{-1} for $Fe(CN)_6^{3-}$ and 2085 cm^{-1} for $Os(CN)_6^{3-}$; the lower energy of the latter clearly indicates the greater importance of back-donation in the osmium complex. Integrated intensity measurements for the two cyanide bands in chloroform solution (10^{-2} *M*) give values of *A* equal to 2.8×10^4 and 5.7×10^4 l. mol^{-1} cm^{-2} for $Fe(CN)_6^{3-}$ and $Os(CN)_6^{3-}$, respectively. These values also indicate[40] a larger degree of back-bonding in the osmium complex.[41] The enhanced participation of π^* in filled orbitals could arise either from the smaller energy difference in the d and π^* diagonal matrix elements in Os than in Fe or from better overlap of the diffuse 5d orbitals with π^*. The two effects are difficult to separate; however, we favor the predominance of the overlap contribution since (a) in the first-row hexacyanides the calculated (and observed) effect of lesser stability of metal orbitals was only to *increase* the energy of the L → M charge transfer; (b) the greater number of nodes in the 4d and 5d orbitals could easily produce more effective overlap with the π^* orbitals of cyanide without raising the σ overlap (and thus increasing Δ greatly; *vide infra*) concomitantly; (c) the observation of Jones[42] from infrared data and our values[27a] of the cyanide stretching frequencies in chloroform point to the conclusion that in the d^6 complexes σ bonding increases in the order Co < Rh < Ir while π^* back-bonding stays about constant (although it would have to increase slightly to prevent ν_{CN} from increasing with σ bonding; in fact, this frequency stays about constant; nevertheless, the order of π^* back-bonding must be Fe > Co and Os > Ir). This could be explained by a contraction of the d orbitals (Os → Ir) to give better σ and worse π^* overlap.

Another observation of interest is the seemingly constant orbital electronegativity displayed by complexes containing the same central metal in two oxidation states. For example, the first M → L band in the Fe(II) complex is at 45,870 and in Fe(III) at 44,000 cm^{-1}; in Mn(II) at 41,000 and in Mn(III) at 41,100 cm^{-1}. Also, in the manganese complexes, the first L → M charge transfer comes at 31,250 and 31,100 cm^{-1}, respectively. This behavior is consistent with our calculations[27] which predict essentially the same charge associated with the central metal for complexes of both II and III oxidation states.

Our observations on L → M charge-transfer bands allow us to construct the following orbital electronegativity series of various metals toward cyanide: Ti(III) < V(III) < Cr(III) < Mn(III) < Fe(III) ~ Ru(III) ~ Os(III).

Δ Values in First-Row Complexes. Table IV presents the spectroscopically derived values of the ligand-field parameters Δ, *B*, *C*, and β. Two features of Δ in cyano complexes of the first row were noted earlier, namely its increase across the series and its slight dependence on oxidation state. This first observation has been accounted for nicely by Jones[40] who showed the increased importance of back-donation with atomic number as evidenced in increased intensity of the M–C stretching bands in the infrared. Such data are consistent with an augmentation of Δ due to increasing participation of cyanide π^* orbitals in the bonding of the complex with accompanying stabilization of the $2t_{2g}$ level *relative* to $3e_g\sigma^*$ in going from Cr to Co.

Table IV. Ligand-Field Parameters for Hexacyanide Complexes

Complex	Δ, cm^{-1}	B_{cpx}, cm^{-1}	$B_{free\ ion}$, cm^{-1}	*C*, cm^{-1}	$\beta = B_{cpx}/B_{free\ ion}$
$Ti(CN)_6^{3-}$	22,300	...	...	...	...
$V(CN)_6^{3-}$	23,500	375	780	2700	0.48
$Cr(CN)_6^{3-}$	26,600	480	845	2670	0.56
$Mn(CN)_6^{3-}$	34,000	660	*a*	3280	*a*
$Mn(CN)_6^{4-}$	30,000	425	900	1800	0.47
$Fe(CN)_6^{3-}$	34,950	720	1090	3290	0.66
$Os(CN)_6^{3-}$	38,000	340	*a*	2000	*a*
$Fe(CN)_6^{4-}$	33,800	380	830	2800	0.45
$Ru(CN)_6^{4-}$	33,800	*a*	*a*	2800	*a*
$Os(CN)_6^{4-}$	>34,000	*a*	*a*	*a*	*a*
$Co(CN)_6^{3-}$	34,500	430	1100	2700	0.39
$Rh(CN)_6^{3-}$	44,000[b]	*a*	*a*	*a*	*a*
$Ir(CN)_6^{3-}$	>45,000	*a*	*a*	*a*	*a*

[a] Insufficient data. [b] From ref 44.

The importance of the M → π^*CN bonding is nicely illustrated on comparing the variation of Δ across the first row (Ti(III) to Co(III)) for the ligands CN^-, F^-, and NH_3. The behavior of Δ for the three types of ligands is in fact quite different, as shown in Figure 8. From Ti(III) to Co(III), the Δ values *decrease* for the π donor F^-, remain virtually *constant* for the non-π-bonding ligand NH_3, and *increase* for the π-acceptor CN^-. Although it is only reasonable that

(38) D. DeFord and A. Davidson, *J. Am. Chem. Soc.*, 73, 1649 (1951).
(39) C. K. Jørgensen, "Orbitals in Atoms and Molecules," Academic Press Inc., New York, N. Y., 1962.
(40) L. H. Jones, *Inorg. Chem.*, 2, 777 (1963).
(41) The integrated intensity values in chloroform seem in general to be somewhat larger than those reported by Jones[40] for water solutions. We find, for example, a value of 4.7×10^4 l. cm^{-2} $mole^{-1}$ for $Co(CN)_6^{3-}$ in $CHCl_3$, while in water Jones reports 1.83×10^4 l. $mole^{-1}$ cm^{-2}.
(42) L. H. Jones, *J. Chem. Phys.*, 41, 856 (1964).

the differences in π-electronic structure of the ligands are responsible for such different behavior, a more subtle point is whether in any given series it is movement of $2t_{2g}$ or $3e_g\sigma^*$ (or both) that gives the Δ trend. Since changes in π bonding factors must necessarily affect σ bonding, it is probable that movement of *both* $2t_{2g}$ and $3e_g\sigma^*$ must be taken into account. Further, we offer that strongly antibonding levels are more sensitive to overlap changes than are nonbonding (or slightly antibonding) ones, and therefore suggest that as the total σ and π d orbital bonding is increased, the Δ gap will widen. Thus at Ti(III), the π donor ligand F^- is capable of strong $\pi F^- \rightarrow M$ bonding; this tends to strengthen the d_σ bonding and give a relatively large Δ. As the $3d^n$ configuration in $2t_{2g}$ builds up, however, F^- suffers increasingly prohibitive interelectronic-repulsion effects and the $\pi F^- \rightarrow M$ bonding drops off. For this reason, in the $3d^6$ case Co(III) a π-donor ligand cannot occupy a position for good overlap with the relatively stable and contracted $3d_\sigma$ orbitals and the Δ value is proportionately smaller. Turning to CN^-, our calculations indicate that π bonding is not a very important contributor to Δ in complexes involving Ti(III) and V(III). As $(2t_{2g})^n$ builds up, however, even the moderate degrees of $M \rightarrow \pi^*CN$ bonding in our estimate are sufficient to allow a significant strengthening of both the d_π and d_σ bonding. Therefore, in sharp contrast to F^-, at Co(III) the CN^- ligand is able to move into a favorable position for overlap with the e_g orbitals. We may thus conclude that, *for a given ligand*, the variation in Δ follows the bond order involving d orbitals. That is, the d-bond order for CN^- increases from Ti(III) to Co(III), decreases for F^-, and stays constant for NH_3; this is precisely reflected in Δ values.

Further evidence that both $2t_{2g}$ and $3e_g\sigma^*$ are affected as the degree of $M \rightarrow \pi^*CN$ bonding changes is provided by the observation that Δ is virtually independent of oxidation state for a given central metal. The fact that the first $M \rightarrow L$ charge-transfer bands occur at approximately the same positions in $Fe(CN)_6^{4-}$ and $Fe(CN)_6^{3-}$ is evidence that $2t_{2g}$ must be stabilized by increased $Fe \rightarrow \pi^*CN$ bonding in the Fe(II) case. And, from our arguments above, the expected drop in $L \rightarrow M$ σ bonding in Fe(II) would not materialize in such a case, with the result that $3e_g\sigma^*$ does *not* undergo any lowering. The combined charge-transfer and ligand-field parameters confirm this picture.

Δ in Second- and Third-Row Complexes. Our observations on the complexes of the second- and third-transition series with d^5 and d^6 configurations point up interesting comparisons between complexes of cyanide and other ligands with regard to the changes in the ligand-field splitting parameter in later transition series. The most prominent feature is the small increase in cyanide Δ's in the Fe-family complexes. In the d^6 complexes, for example, we have $\Delta[Fe(CN)_6^{4-}] \approx \Delta[Ru(CN)_6^{4-}]$. Data for various d^5 systems are not complete down a whole family, but it is clear that the increase of Δ from 35,000 cm^{-1} in $Fe(CN)_6^{3-}$ to 38,000 cm^{-1} in $Os(CN)_6^{3-}$ is considerably smaller than would be anticipated for ammine and halide complexes.[32,43]

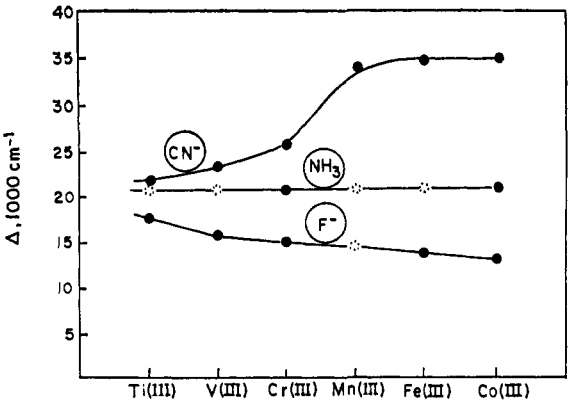

Figure 8. Variations of Δ with metal for the ligands CN^-, NH_3, and F^-. Data are taken from the following sources: cyano complexes, from this work; fluoro complexes, from H. Basch, A. Viste, and H. B. Gray, *J. Chem. Phys.*, **44**, 10 (1966); ammine complexes, from ref 30. Dotted circles are estimated values.

We pointed out earlier that this slow increase in Δ down an *n*d series can be interpreted as coming entirely from increasing stabilization of $2t_{2g}$; indeed, the evidence is strong that in the series Fe–Ru–Os no enhancement of d orbital σ bonding takes place in hexacyano complexes as *n* increases from 3 to 5. The increased number of nodes may favor $d \rightarrow CN\pi^*$ bonding, but, at the relatively short M–(CN) distances characteristic of significant π bonding, the presence of more nodes apparently works against σ bonding to a relatively expanded set of e_g orbitals. This effect is most pronounced in metal hexacarbonyl complexes and will be elaborated on further in a forthcoming paper.[43]

In contrast to the Fe-family complexes, the hexacyanides of Co(III), Rh(III), and Ir(III) display a rather large increase in Δ in the order $3d < 4d < 5d$. Specifically, we have $\Delta[Co(III)] = 34{,}500$, $\Delta[Rh(III)] = 44{,}000$,[44] and $\Delta[Ir(III)] > 45{,}000$ cm^{-1}. These results are in agreement with the previous conclusion from infrared data that, for these more contracted e_g orbitals, σ bonding shows an increase in the expected order $3d < 4d < 5d$.

Acknowledgments. Miss Paula Jacoby kindly performed several infrared measurements. We thank the National Science Foundation for support of this research. In addition, we are grateful to the Institute for Space Studies for the usage of computer facilities.

(43) N. A. Beach and H. B. Gray, *J. Am. Chem. Soc.*, in press.
(44) H.-H. Schmidtke, *Z. Physik. Chem.* (Leipzig), **40**, 96 (1964).